Cu CLUSTERING AND Si PARTITIONING IN THE EARLY CRYSTALLIZATION STAGE OF AN $Fe_{73.5}Si_{13.5}B_9Nb_3Cu_1$ AMORPHOUS ALLOY

K. HONO, D. H. PING, M. OHNUMA AND H. ONODERA
National Research Institute for Metals, 1-2-1 Sengen, Tsukuba 305-0047, Japan

Abstract - Solute clustering and partitioning behavior in the early crystallization stage of an $Fe_{73.5}Si_{13.5}B_9Nb_3Cu_1$ amorphous alloy have been studied by employing a three dimensional atom probe (3DAP) and a high resolution electron microscope (HREM). 3DAP results have clearly shown that Cu atom clusters are present in the amorphous state after annealing below the crystallization temperature. The density of these clusters are in the order of 10^{24} m^{-3}, which is comparable to that of the α-Fe grains in the optimum nanocrystalline microstructure. In the early stage of primary crystallization, Cu clusters are in direct contact with the α-Fe nanocrystals, suggesting that each α-Fe primary particles are heterogeneously nucleated at the site of Cu clusters. In the early stage of crystallization, the concentration of Si is lower in the primary crystal than in the amorphous matrix phase, unlike in the late stage of the primary crystallization, where Si partitions into the α-Fe phase with a composition of approximately 20 at.%.

1. INTRODUCTION

A nanocrystalline Fe-Si-B-Nb-Cu alloy, known as FINEMET, is a very attractive soft magnetic material exhibiting excellent permeability while maintaining a high saturation magnetization [1-2]. This material is prepared by annealing a melt-spun $Fe_{73.5}Si_{13.5}B_9Nb_3Cu_1$ amorphous ribbon at temperatures in the range of 520 - 580°C. The microstructure produced by the primary crystallization reaction consists of nanoscale α-Fe grains embedded in the remaining amorphous matrix. The average grain size is approximately 10 nm, and the grains are randomly oriented without having any preferred orientation. The random orientation of the nanoscale grains are attributed to reduction in the net magnetocrystalline anisotropy, resulting in high permeability [3].

In the optimum noncrystalline microstructure which gives rise to the best soft magnetic property (after 60 min annealing at 550°C), three distinct phases were identified [4-6]. One is α-Fe nanocrystals containing approximately 20 at.%Si. Mössbauer spectroscopy work [7] and more recent selected area electron diffraction (SAD) results [8] suggested that the α-Fe phase is ordered to the DO_3 structure (Fe_3Si). However, because of its offstoichiometric composition, the DO_3 ordered reflections are barely observable by SADP, and X-ray diffraction does not provide sufficient intensity for the DO_3 ordered structure [8]. In this paper, this phase is simply designated as α-Fe regardless of its ordered state or the content of Si, because α-Fe form the primary solid solution with Si in a wide range of solubility and ordering to the DO_3 structure is of the second order transition. These α-Fe nanocrystals are embedded in the amorphous matrix which are enriched with Nb and B. The concentration of Nb and B were estimated to be approximately 10 and 15 at.% by atom probe field ion microscopy (APFIM) [4]. The last phase is the fcc-Cu, whose composition is probably close to 100 at.%, and the size is approximately 5 nm [5].

The mechanism of such nanocomposite microstructure evolution has been a subject of numerous studies. Earlier APFIM studies by Hono et al. [6] reported that Cu atoms form clusters prior to the onset of the crystallization reaction. In the optimum microstructure, Cu atoms form fcc-Cu precipitates of approximately 5 nm. These observations suggested that Cu clustering stimulates nucleation of the α-Fe primary particles in the crystallization stage. However, no direct evidence for the Cu clusters serving as heterogeneous nucleation sites for the α-Fe particles have been presented in the previous work. Cu particles were observed spatially separated from the α-Fe particle in the one dimensional atom probe concentration depth profile [5].

From extended x-ray absorption fine structure (EXAFS) measurement results, Kim et al. [9] and Ayers et al. [8, 10-12] reported that Cu atoms

form clusters with near-fcc symmetry from very early stage of the heat treatment, with some evidence of their presence even in the as-melt-spun amorphous alloy. Ayers et al. [8, 12] proposed that Cu clusters which form in the amorphous matrix provide nucleation sites for the α-Fe primary particles, and subsequently Cu clusters are enveloped by the α-Fe nanocrystals in the optimum microstructure. The assumption that Cu clusters serve as heterogeneous nucleation sites for the a-Fe primary crystals is quite reasonable, but direct evidence for this mechanism is very difficult to obtain because the sizes of the Cu clusters and the primary particles are both extremely fine. However , in the case of a nanocrystalline Fe-Zr-B-Cu alloy, Cu clusters were found in intimate contact with the primary α-Fe particles by APFIM [13], and analogous situation is expected in the Fe-Si-B-Nb-Cu system as well. Although the earlier APFIM and EXAFS investigations convincingly showed presence of Cu clusters prior to the onset of the crystallization reaction in the Fe-Si-B-Nb-Cu amorphous alloy, how Cu clusters stimulate nucleation of the α-Fe has been a mere speculation.

The aim of this paper is to report definite new experimental results by 3DAP and HREM concerning the role of Cu clustering to nanocrystallization of a Fe-Si-B-Nb-Cu amorphous alloy. In addition, peculiar partitioning behavior of Si in the early crystallization stage is reported.

2. EXPERIMENTAL

A melt-spun $Fe_{73.5}Si_{13.5}B_9Nb_3Cu_1$ amorphous ribbon was kindly provided from Dr. Yoshizawa of Hitachi Metals Co. Ltd. The thickness of the ribbon specimen was approximately 20 μm. These as-melt-spun ribbons were annealed at 400, 450, 500 and 550 °C for 5, 10 and 60 min in high vacuum. Thin foil specimens for TEM observations were prepared by ion milling from both sides of the ribbon. Conventional TEM observations were made by Philips CM200. High resolution electron microscopy (HREM) observations were carried out by JEM-4000EX, whose point to point resolution is 0.17 nm. Specimens for atom probe analysis were prepared by mechanically grinding the ribbon to a square rod of approximately 20 μm x 20 μm x 6 mm followed by micro-electropolishing to a sharp needle shape specimen. These specimens were observed by field ion microscope (FIM) and then analyzed by a three dimensional atom probe (3DAP). The 3DAP was equipped with CAMECA's tomographic atom probe (TAP) detection system [14] which was installed to a locally designed FIM chamber. The atom probe

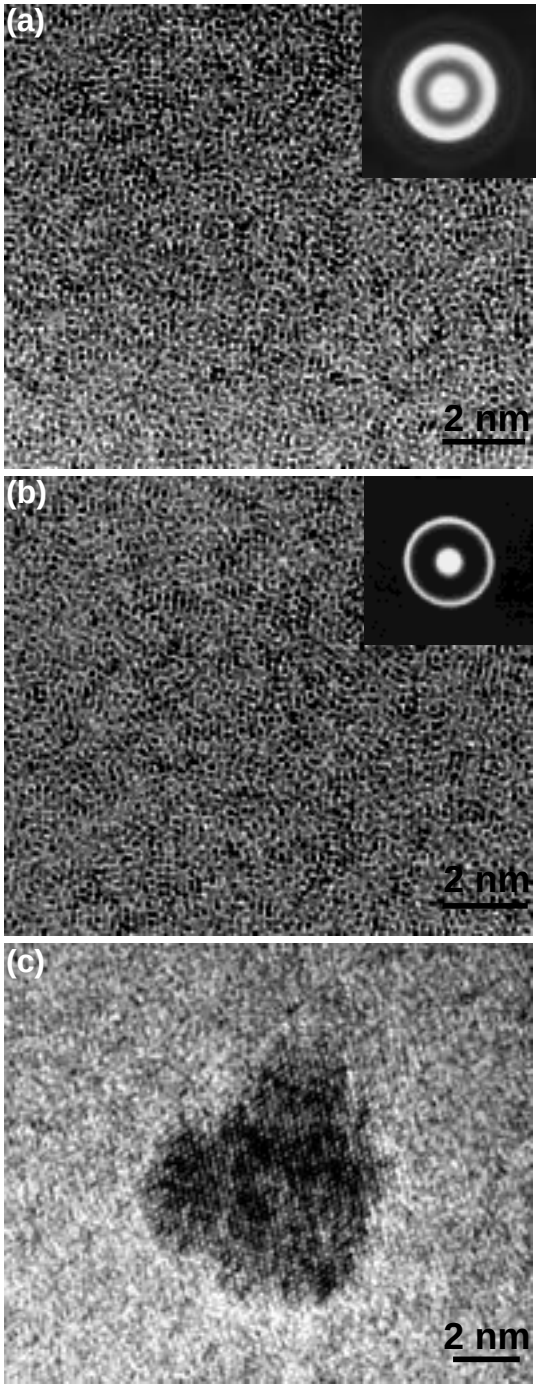

Fig. 1 HREM images and SADP of melt-spun Fe-13.5Si-9B-3Nb-1Cu alloy ribbon (a) as-quenched, (b) annealed for 60 min at 400°C, and (c) annealed for 5 min at 450°C.

analyses were performed with a pulse fraction (V_p/V_{dc}) of 0.2 and a pulse repetition rate of 600 Hz at a specimen temperature of 35 K under an ultrahigh vacuum of ~$1x10^{-8}$ Pa. The data analysis and visualization of 3DAP data were carried out using KINDBRISK SDV and SSA 3DAP data analysis software under Advance Visualizaiton System (AVS).

3. RESULTS

3.1 HREM observation

HREM images of as-melt-spun specimen, specimens annealed at 400 °C for 60 min and annealed at 450 °C for 5 min are shown in Fig. 1 (a), (b) and (c), respectively. The HREM image of the as-melt-spun specimen (Fig. 1(a)) shows isotropic maze contrast typical for an amorphous structure. The selected area diffraction pattern (inset figure) exhibits typical halo ring suggesting that the as-melt-spun specimen is amorphous. The HREM image of the specimen annealed at 400 °C for 60 min shows similar image feature of the amorphous structure. No recognizable difference is observed in the selected area diffraction pattern, either. This suggests that annealing at 400 °C as long as 60 min does not induce primary crystallization of α-Fe phase. After 5 min annealing at 450 °C, nanometer scale (~7 nm) grains of primary α-Fe crystal has been recognized as shown in fig. 1(c). Although 450 °C is still lower than the crystallization temperature, ~517 K, determined by DSC with a heating rate of 10 K/min [2], crystallization does occur by isothermal heat treatment as long as 5 min. On the other hand, no evidence for primary crystallization has been observed at 400 °C, thus the specimens annealed at 400°C for 60 min has been examined by 3DAP for investigating pre-crystallization clustering of Cu atoms. For investigating local chemical changes in the early crystallization stage, specimens annealed at 450, 500 and 550 °C has been analyzed by 3DAP.

3.2 Atom probe analysis of pre-crystallization clustering

Figures 2 (a), (b) and (c) show 3DAP elemental mappings of Cu within analyzed volumes of 10 x 10 x 40 nm in the as-melt-spun specimen, in the specimens annealed for 5 and 60 min at 400°C, respectively. In the as-melt-spun specimen, Cu distribution is uniform. The other solute elements have also been found to be uniformly distributed (not shown in the figure),

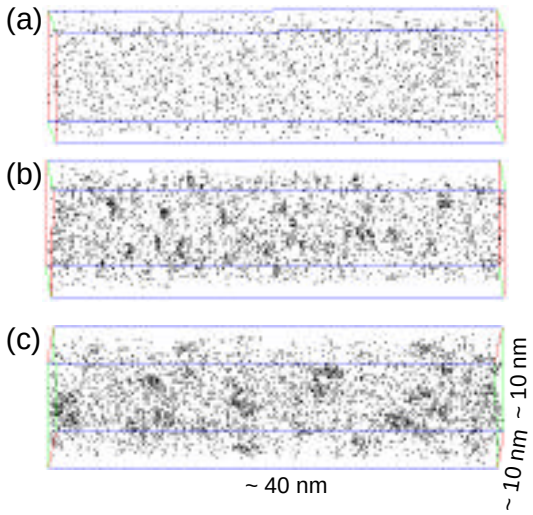

Fig.2 3DAP elemental mapping of Cu of melt-spun Fe-13.5Si-9B-3Nb-1Cu alloy ribbon (a) as-quenched, (b) annealed for 5 min at 400°C, and (c) annealed for 60 min at 400°C.

confirming that the as-melt-spun specimen is chemically homogeneous solid solution with the amorphous structure. In the specimen annealed for 5 min at 400 °C, inhomogeneous distribution of Cu atoms is apparent, indicating that clustering of Cu atoms occurs. After 60 min annealing at 400°C, clustering is more clearly observed. The number of atoms in each clusters is in the range of 50 to 100 (taking the detection efficiency of the microchannel plate detector into consideration) and the size of the clusters is approximately 3 nm. The structure of these clusters are unknown, as HREM image does not give fringe contrast corresponding to any crystalline structure. The density of the Cu clusters estimated from the analyzed volume is in the order of 10^{24} m^{-3}. The concentration of the Cu cluster has been estimated to be approximately 12 at.% Cu.

Figure 3 (a) shows solute atom distributions near a Cu cluster in a specimen annealed at 400°C for 60 min. It appears that there are no correlation between Cu atoms and the distributions of the other solutes, Nb, B and Si. Figure 3 (b) shows concentration depth profiles obtained across the Cu cluster. The Fe concentration profile shows that Cu enrichment cause only reduction in Fe concentration without affecting concentrations of Nb and B. From this observation, it is concluded that Nb and B are not correlated with clustering of Cu. This result is similar to atom probe results of Cu clustering in Fe-Zr-B-Cu alloy [14], where only concentration

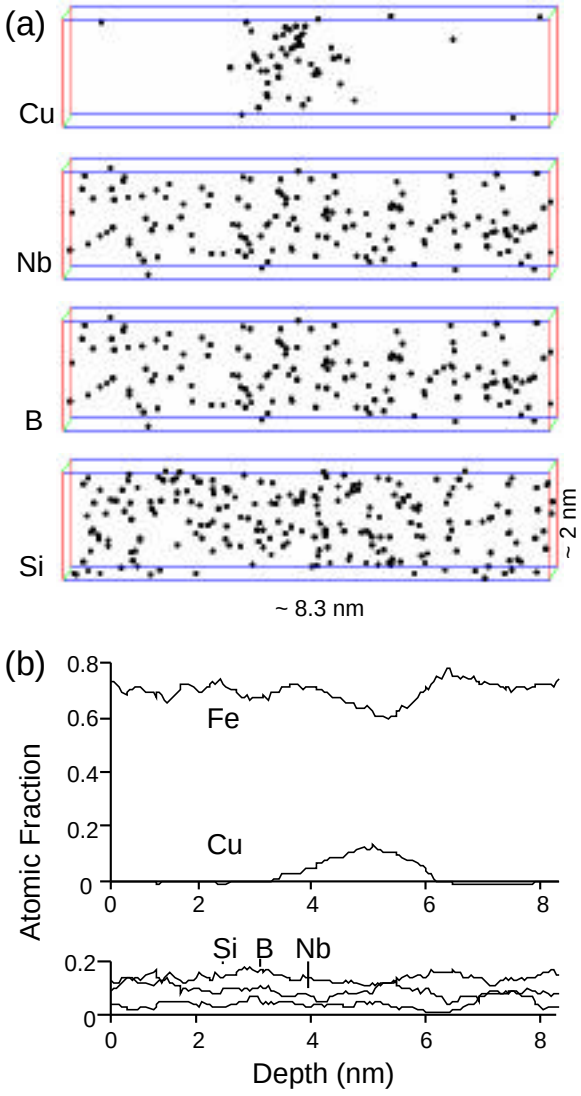

Fig.3 (a) 3DAP elemental mappings of Cu, Nb, B and Si atoms near a Cu cluster in a melt-spun Fe-13.5Si-9B-3Nb-1Cu alloy annealed for 60 min at 400°C and (b) the corresponding concentration depth profiles obtained from the same analyzed volume.

of Fe was found to be affected by clustering of Cu.

3.3 Atom probe analyses of crystallized microstructure

Distribution of Cu atoms in a selected volume of the specimen annealed at 450°C for 5 min is shown in Fig. 4 (a) and iso-concentration surface of 20 at.%Cu is shown in Fig. 4 (b). As shown in Fig. 1 (c), sparsely dispersed small primary crystals are present in this specimen, thus this

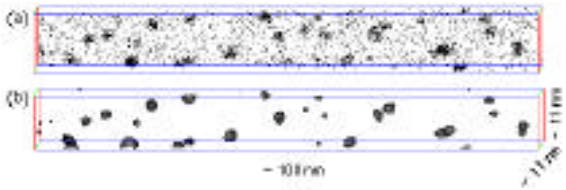

Fig.4 (a) 3DAP elemental mapping of Cu atoms in a melt-spun Fe-13.5Si-9B-3Nb-1Cu alloy annealed for 10 min at 450°C, and (b) the corresponding iso-concentration surface of 20 at.%Cu. The number density of the clusters is estimated to be ~10^{24} /m^3.

stage is categorized as the nucleation-and-growth stage of the primary crystal. The density of the Cu enriched particles is in the order of 10^{24} m^{-3}, which is same as that in the amorphous specimen annealed for 60 min at 400°C. The concentration of Cu of these were estimated to be approximately 70 at.%, which is significantly higher than that in the amorphous specimen annealed for 60 min at 400°C.

Fig. 5 (a) shows 3D elemental maps near a Cu precipitate in the Fe-13.5Si-9B-3Nb-1Cu alloy annealed at 550°C for 10 min. In this figure, the interface between α-Fe and amorphous phases is clearly seen from the drastic change in concentrations of B and Nb. The densities of Nb and B are higher in the remaining amorphous phase, while they are lower in the α-Fe. Cu precipitate is at the interface and it is direct contact with the α-Fe particle, which suggests that Cu provides nucleation sites for the α-Fe primary crystals. The concentration depth profile along the selected volume is shown in Fig. 5 (b). The partitioning of solutes are in good agreement with the previous report using a conventional atom probe [5]. As Nb and B are enriched in the remaining amorphous phase being rejected from the α-Fe primary particles, it is possible to show amorphous region by drawing isoconcentration surfaces in the 3DAP data. Figure 6 shows distribution of Cu atoms and isoconcentration surface constructed by connecting Nb and B enriched regions. The region surrounded by the isosurface corresponds to the amorphous phase, and the other region correspond to the α-Fe phase. It appears that each Cu precipitate is located in contact with each α-Fe particles. This result again support that Cu precipitates (or clusters) directly serve as heterogeneous nucleation sites for the α-Fe primary crystals.

3.4 Si partitioning in α-Fe

Figure 7 (a) and (b) show atom probe concentration depth profiles obtained from the specimens annealed at 450°C for 10 min and 550°C for 60 min. After 10 min annealing at 450°C, a primary α-Fe crystal can be observed as indicated in Fig. 7 (a), from which both Nb and B are depleted. Significant change in Si concentration cannot be observed, but it appears that Si atoms are also slightly depleted from the primary α-Fe particle. Pile up of Nb atom can be seen at one of the α-Fe/amorphous interfaces as indicated by an arrow. After annealing for 60 min at 550°C, Si is enriched in the α-Fe phase and its concentration in the remaining amorphous phase is lower than that in the α-Fe phase. This result is consistent with our earlier report [5]. Note also that Nb is completely rejected from the α-Fe phase, while a few atomic percent of B remaining. More quantitative description of the partitioning of each solute are shown as integrated concentration profile as shown in Fig. 7 (c) and (d). Annealing at 450°C for 5 min lead to almost complete depletion of Nb from the α-Fe particle (0.3 at.%), but approximately 2.3 at.% of B is still resolved in the α-Fe phase. Si concentration is lower in the

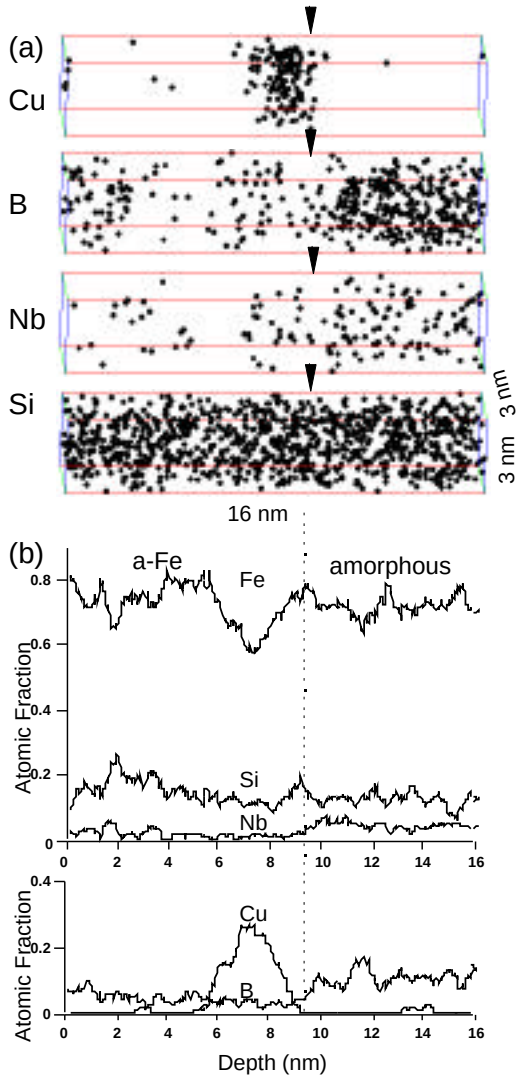

Fig. 5 (a) 3DAP elemental mappings of Cu, B, Nb and Si atoms near a Cu precipitate in a selected volume of a melt-spun Fe-13.5Si-9B-3Nb-1Cu alloy annealed for 10 min at 500°C. (b) Concentration depth profiles of Fe, Si, Nb, B and Cu in the selected volume.

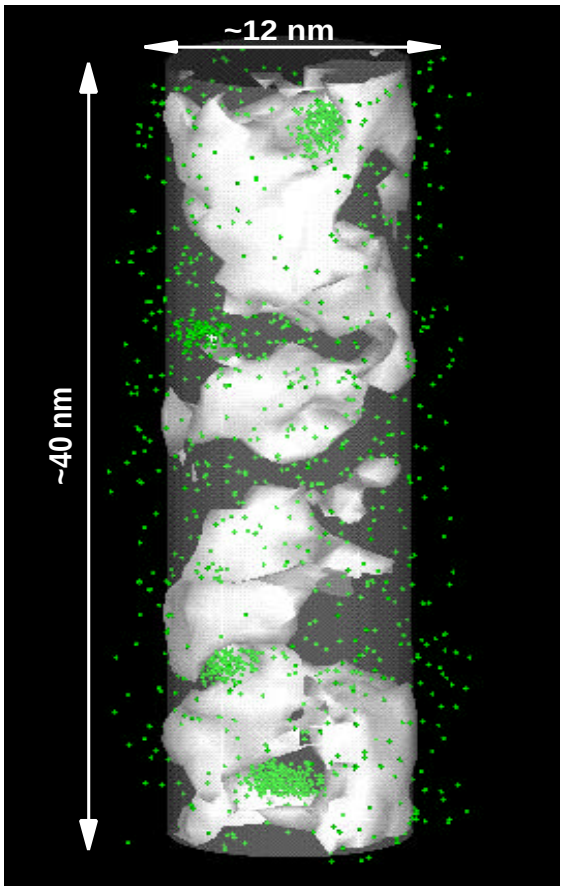

Fig. 6 Distribution of Cu atoms superimposed on isoconcentration surfaces showing Nb and B enriched amorphous phase in a melt-spun Fe-13.5Si-9B-3Nb-1Cu alloy annealed for 10 min at 500°C.

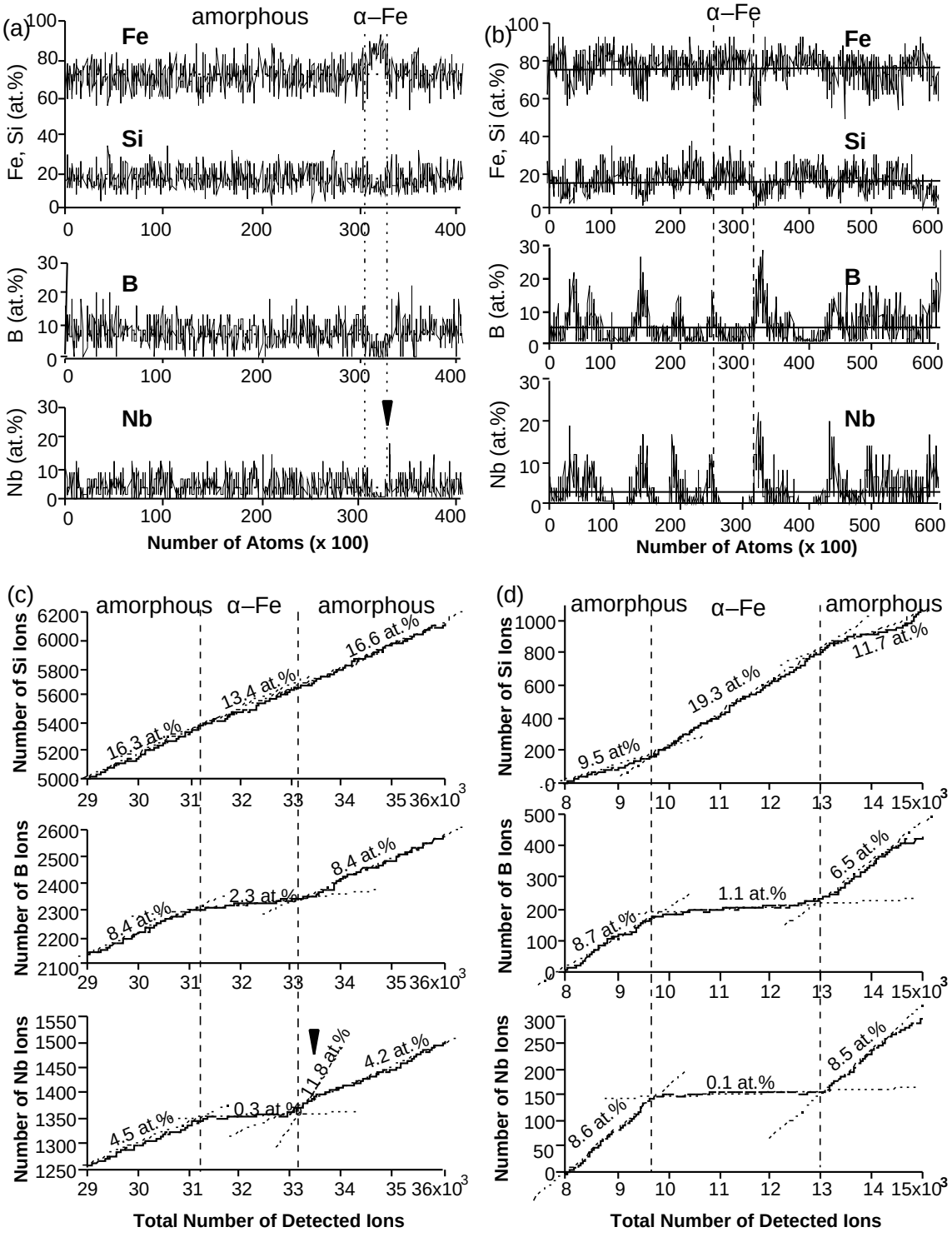

Fig. 7 One dimensional atom probe concentration depth profiles of melt-spun Fe-13.5Si-9B-3Nb-1Cu alloy (a) annealed at 450°C for 10 min and (b) annealed at 550°C for 60 min. Integrated concentration depth profiles (ladder diagrams) from selected regions of melt-spun Fe-13.5Si-9B-3Nb-1Cu alloys (c) annealed at 450°C for 10 min and (d) annealed at 550°C for 60 min.

phase (~16 at.%). After annealing for 60 min at 550 °C, Si is preferentially partitioned into the residual amorphous phase (~19 at.%) with a partitioning factor larger than 2. Nb concentration in the α-Fe is almost zero, while ~1.0 at.% of B still remain. This result indicates that Si partitioning to the α-Fe progress as the particle grows, and the concentration of Si in the nuclei of the α-Fe is significantly lower than that in the final microstructure.

4. DISCUSSION

4.1 Role of Cu as nucleation agent

This study has unambiguously shown that Cu clusters form in the amorphous state prior to the onset of the crystallization reaction. During the clustering process, Cu atoms substitute for Fe atoms and their clustering does not affect distribution of the other solutes. The concentration of Cu in the clusters is significantly lower than the equilibrium value for the ε-Cu at the beginning, but it increases as it grows. Some of the Cu clusters were observed in direct contact with the α-Fe primary particles, suggesting that the Cu clusters serve as heterogeneous nucleation sites for the primary crystals. The density of the Cu clusters observed in the amorphous state was in the range of 10^{24} m^{-3}. Assuming that the grain size of the α-Fe in the optimum microstructure is 10 nm with a volume fraction of 70% [17], the density of the α-Fe is estimated to be 1.3 x 10^{24} m^{-3}. Thus, the density of the Cu clusters and that of the α-Fe nanocrystals are comparable, and thus, the nanocrystalline microstructure can be formed even if they are all nucleated by the heterogeneous nucleation at the site of the Cu clusters. In fact, the 3DAP data obtained from a larger volume shown in Fig. 6 demonstrate that Cu cluster is present corresponding to each α-Fe particle.

This conclusion is different from our earlier proposed mechanism for the nucleation of the α-Fe which was based on the conventional atom probe data [5]. The conventional AP corrects atoms from a cylindrical volume covered by the probe hole from the surface to the depth using field evaporation, and it determines local concentration based on the number of corrected atoms. Thus, one dimensional concentration profile is obtained from the region covered by the probe hole. Even if Cu clusters are adjacent to the α-Fe primary particles, the one dimensional concentration depth profile may not show the Cu cluster in direct contact with the primary phase unless the cylindrical volume cut these particles with an appropriate geometry. The chance of obtaining such an ideal concentration depth profile is low by 1DAP, but one of such rare examples was found in Cu clusters in Fe-Zr-B nanocrystalline softmagnetic material [13]. Small sampling volume is also a limitation of the conventional atom probe. The present investigation has clearly demonstrated that larger volume of analysis made possible by 3DAP is more suitable for obtaining accurate information on morphology of the microstructure.

The direct observation result of Cu clusters providing heterogeneous nucleation site of the α-

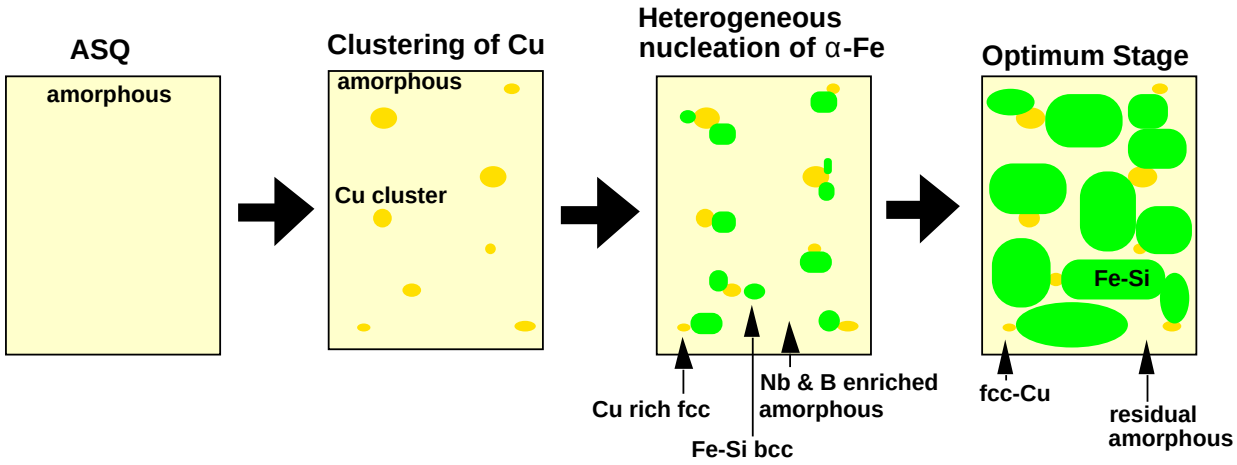

Fig. 8 Schematic drawing of microstructural evolution in melt-spun Fe-13.5Si-9B-3Nb-1Cu amorphous alloy by primary crystallization.

Fe primary crystals supports the model recently proposed by Ayer et al. [8]; however, the present results indicate that the actual microstructure is slightly different from their model. We found Cu clusters at the interface of the remaining amorphous phase and the α-Fe phase. This strongly suggests that the α-Fe do not envelope Cu particles after growth. Based on the present results, the nanocrystallization process of this alloy can be schematically presented as shown in Fig. 8. Initial amorphous phase is chemically uniform amorphous solid solution. By annealing, Cu clusters appear in the fully amorphous matrix. The structure of the Cu cluster has not been determined by the present study, but it is believed that these clusters have the fcc-like short range structure according to EXAFS results [8]. The concentration of Cu of the cluster is significantly lower (~20at.%) than the equilibrium fcc ε-Cu, thus, it is unlikely that the clusters have the distinct fcc structure at this stage. As Cu time goes on, the concentration of Cu in the cluster increases, and their structure become more like fcc. By further annealing, the primary crystals of the α-Fe are heterogeneously nucleated at the Cu/amorphous interfaces. In the final microstructure, the fcc-Cu particles are present in direct contact with the α-Fe grains, but they are not entirely enveloped by the α-Fe phase.

The reason why Cu clusters provide heterogeneous nucleation site can be explained as follows. According to Kim et al [9] and Ayers et al. [8,10-12], the Cu particle has the nearest neighbor structure similar to the fcc-Cu. Initially, as the Cu concentration of the clusters are lower, their structural feature will be limited only in the short range. As they grow, the clusters would have more distinct feature as the fcc structure. It is known that $(111)_{fcc\text{-}Cu}$ and $(011)_{bcc\text{-}Fe}$ has very good matching, thus $(111)_{fcc\text{-}Cu}$ would provide low interfacial energy if α-Fe is nucleated on this surface with either Nishiyama-Wasserman or Kurdjumov-Sachs orientation relationship (OR). In addition to such structural factor, there would be a chemical factor to enhance nucleation of α-Fe at the Cu cluster interface. As the atom probe data has shown, Cu atoms substitute for Fe atoms when they form clusters. Thus, Fe atoms are rejected from the Cu clusters and would be piled-up at the Cu/amorphous interface. Then, heterogeneous nucleation at the Cu/amorphous interface would be chemically more favorable than homogeneous nucleation inside the amorphous phase.

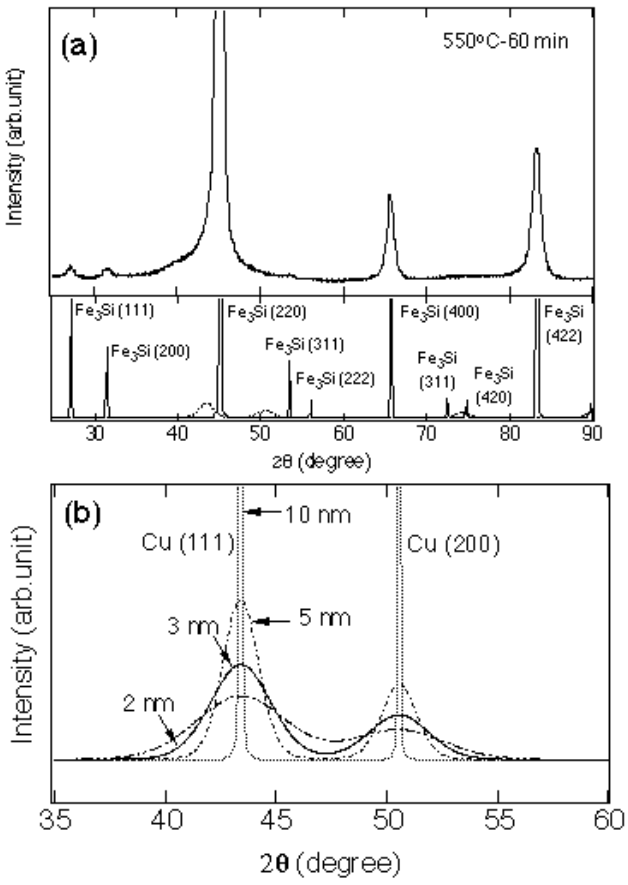

Fig. 9 (a) X-ray diffraction results of Fe-13.5Si-9B-3Nb-1Cu annealed at 550°C for 60 min. Simulated diffraction intensity is shown in the inset. (b) X-ray diffraction intensity expected from various sizes of fcc-Cu particles.

While the DO_3 ordering spot can be clearly recognized in x-ray diffraction profile from the optimum microstructure as shown in Fig. 9, no diffraction spots corresponding to the fcc-Cu can be seen. Cu reflections are not recognized even by the SAD technique, while they were detected by the nanobeam diffraction method [6]. This can be explained from the small size of the particles. The grain size of the fcc-Cu in the optimum microstructure is approximately 5 nm, and this cause broadening of diffraction intensity due to the size effect. Fig. 9 (b) simulate the variation of the intensity of the x-ray diffraction depending on the particle size. When the size of the fcc-Cu is smaller than 5 nm, the diffraction peaks are significantly broadened and the intensity decreases accordingly. When Cu particles less than 5 nm is dispersed in the microstructure composed of 10 nm α-Fe

particles and residual amorphous phase, the diffraction intensity from the fcc-Cu would be totally undetectable.

4.2 Partitioning of Si in α-Fe

It was reported that Si partitions into the α-Fe in the optimum microstructure, forming the DO_3 ordered structure. The concentration of Si in the α-Fe phase was estimated to be approximately 20 at.% in many previous investigates [5,7,15], and the result of this work is consistent with these. In their recent work, Ayers et al. [8] reported that the primary particles have the DO_3 structure from the nucleation stage. However, they observed clear DO_3 feature in their EXAFS results only after 4 min annealing, and pointed out the possibility of incomplete ordering in the initial stage. In terms of this, the lower concentration of Si in the crystallites observed by the present APFIM study in the early stage crystallization at 400°C is particularly interesting. Si does not partition in the α-Fe from the very early stage. Rather, the concentration of Si in the α-Fe appears to be lower than in the amorphous matrix at the beginning. Thus, we can conclude that Si partitioning occurs during the growth stage, not at the nucleation stage. Then, the initial nuclei of the α-Fe would have much lower degree of order than the α-Fe in the optimum microstructure, because its composition is highly offstoichiometric from that of Fe_3Si. This could be the reason for incomplete ordering observed by Ayers et al. by EXAFS [8].

Our recent studies of Si partitioning in Fe-Zr-B nanocrystalline alloy [16] convincingly demonstrated that Si does not partition into the α-Fe phase, but it does partition in the remaining amorphous phase. Our more recent studies on Fe-7Nb-3B-4Si nanocrystalline alloy [17] also demonstrated that Si does not partition in the α-Fe phase, but does in the remaining amorphous phase. These observation results suggest that Si does not have strong driving force to partition into the α-Fe phase. Si has strong affinity with Zr or Nb, thus Si tend to be attracted where Zr or Nb is enriched. This is why Si is enriched in the remaining amorphous phase in Fe-7Zr-3B-4Si and Fe-7Nb-3B-4Si amorphous/nanocrysalline composites. In the case of the FINEMET alloy, Si content is much higher and Nb content is much lower than those in Fe-7Zr-3B-4Si and Fe-7Nb-3B-4Si alloys. Thus, more Si is available than is attracted with Nb. Thus, excess Si would dissolve in the α-Fe, because the solubility of Si in the α-Fe is very large. It is interesting to note that complete ordering to the DO_3 structure on crystallization was reported in the alloy without Nb [8]. This suggests that Si is partitioned into the α-Fe phase from the initial stage of crystallization without Nb, resulting in formation of the DO_3 structure from the nucleation stage. However, under the presence of Nb, Si is initially depleted form the α-Fe phase, probably because it is dragged with Nb to the remaining amorphous phase at the beginning. This work has demonstrated that partitioning behavior of Si varies depending on its composition, temperature and annealing time.

5. CONCLUSIONS

3DAP analysis of various stages of crystallized microstructures of the Fe-13.5Si-9B-3Nb-1Cu alloy (FINEMET0 has given more complete information on the microstructural feature compared to the earlier conventional atom probe work. Following facts have revealed in the present study.

(1) Cu clustering occurs prior to the onset of the primary crystallization reaction. The density of the clusters is in the order of 10^{24} m^{-3}.

(2) These Cu clusters serve as heterogeneous nucleation sites for the primary crystallization of the α-Fe.

(3) Si concentration in the α-Fe phase in the very early crystallization stage is lower than that in the final microstructure.

Acknowledgements —We thank Dr. Yoshizawa of Hitachi Metals Inc., for provision of the specimen used in the present study. This work is partly supported by New Energy Industrial Development Organizaiton (NEDO) International Joint Research Grant.

REFERENCES

1. Yoshizawa, Y., Oguma, S. and Yamauchi, K., J. Appl. Phys., 1988, **64**, 6044.
2. Yoshizawa, Y. and Yamauchi, K., Mater. Trans. JIM, 1990, **21**, 307.
3. Herzer, G., IEEE Trans. Mag., 1989, **25**, 2227.
4. Hono, K., Inoue, A. and Sakurai, T., Appl. Phys. Lett. 1991, **58**, 2180.
5. Hono, K., Hiraga, K., Wang, Q., Inoue, A. and Sakurai, T., Acta metall. mater. 1993, **40**, 2137.

6. Hono, K., Li, J-L., Ueki, Y., Inoue, A. and Sakurai, T., Appl. Surf. Sci. 1993, **67**, 398.
7. Pundt, A., Hampel, G. and Hesse, J., Z. Phys. B, 1992, **87**, 65.
8. Ayers, J. D., Harris, V. G., Sprague, J. A., Elam, W. T. and Jones, H. N., Acta Meter., 1998, **46**, 1861.
9. Kim, S. H., Matsuura, M., Sakurai, M. and Suzuki, K., Jpn. J. Appl. Phys. 1993, **32**, 676.
10. Ayers, J. D., Harris, V. G., Sprague, J. A. and Elam, W. T., IEEE Trans. Mag. 1993, **29**, 2664.
11. Ayers, J. D., Harris, V. G., Sprague, J. A. and Elam, W. T., Appl. Phys. Lett. 1994, **64**, 974.
12. Ayers, J. D., Harris, V. G., Sprague, J. A., Elam, W. T. and Jones, H. N., NanoStructured Mater. 1997, **9**, 391.
13. Hono, K. and Sakurai, T. Sci. Rep. RITU, 1997, **A44**, 223.
14. Blavette, D., Deconihout, B., Bostel, A., Sarrau, J. M., Bouet, M. and Menand, A., Rev. Sci. Instrum, 1993, **64**, 2911.
15. Müller, M., Mattern, N. and Illgen, L., Z. Metallkde., 1991, **82**, 895.
16. Zhang, Y., Hono, K., Inoue, A. and Sakurai, T., Scripta Metall. Mater., 1996, **34**, 1705.
17. Ping, D. H. and Hono, K. and Inoue, A., unpublished work.